

Research Journal of Pharmaceutical, Biological and Chemical Sciences

Sintering and Dielectrics Properties of PZT-PMI Ferroelectric Ceramics Doped with La_2O_3 .

Malika Abba^{1*}, Ahmed Boutarfaia², Necira Zelikha², Abdessalem noura²,
Meklid Abdelhek², and Bounab Karima².

¹Laboratory of Molecular Chemistry and environment, Departement of Science Matter, university of Biskra, BP.145, RP-Biskra(07000), Algeria

²Laboratoire de chimie appliquée (LCA), département des science de la matière, Université de Biskra, Algérie.

ABSTRACT

The effect of La_2O_3 additions on the microstructure and dielectric properties of the $\text{Pb}_{0.95}\text{La}_{0.05}[\text{Zr}_x\text{Ti}_{(0.95-x)}](\text{MO}_{1/3}, \text{In}_{2/3})_{0.05}]_{0.9875}\text{O}_3$ (x ranged from 0.46 to 0.55) ceramics have been investigated. All of the samples were prepared by conventional solid state process. The results of X-ray diffraction showed that all the ceramics specimens have a perovskite phase. In the present system, the MPB that coexists with the tetragonal and rhombohedral phases is a narrow composition region of $x = 0.50 - 0.51$. A sintered density of 98.50% of the theoretical density was obtained for Zr = 50% after sintering at 1150°C. Ceramics sintered at 1150°C with Zr = 50% achieve excellent dielectric properties, which are as follows $\epsilon_r = 5413.583$, $\tan\delta = 0.0392$ and $T_c = 335^\circ\text{C}$.

Keywords: MPB, Sintering, Dielectric properties, Zr/Ti ratio.

**Corresponding author*

INTRODUCTION

Lead zirconate titanate (PZT) solid solutions of the ABO_3 perovskite type structure (where A- sites are occupied by Pb^{2+} ions and B-sites by Zr^{4+} and Ti^{4+} ions) show excellent piezoelectric properties. Near morphotropic phase boundary (MPB) lead zirconate titanate $Pb(Zr Ti)O_3$ (PZT) is a binary solid-solution of $PbTiO_3$ ferroelectric and antiferroelectric $PbZrO_3$ [1]. The most commonly used ceramics $Pb(Zr_x Ti_{1-x})$ had a composition closed to the MPB at $x \sim 0.52$ [1-3], where properties such as piezoelectric coefficients and dielectric permittivity are maximized. Classically, the electrical properties of PZT ceramics are modulated by the incorporation of small amounts of cations (doping) (typically 0.5 -2 mole %). Modification of PZT with suitable substitutions of single or multiple cations at Pb^{2+} and Zr^{4+}/Ti^{4+} sites helps in enhancing its physical and electrical properties[4-6]. Dopants are classified as acceptors or donors [7]. Acceptors (monovalent at A site and trivalent at B site) introduces oxygen vacancies to maintain charge neutrality and this caused lower dielectric constant and losses (at room temperature). Donors (trivalent ion at A site and pentavalent ion at B site) reduces the concentration of intrinsic oxygen vacancy and cause the following changes of the characteristics of PZT: higher dielectric constant and losses (at room temperature).

The influence of technological factors on the width of the co-existence region was investigated on the ternary system $Pb_{0.95}La_{0.05}[Zr_xTi_{(0.95-x)}(Mo_{1/3},In_{2/3})_{0.05}]_{0.9875}O_3$ by X-ray diffraction by varying the ratio Zr/Ti. The purpose of this work is to study the influence of sintering temperature on density of the ceramic in order to determine the width of co-existence of tetragonal and rhombohedral phases and the exact composition of the MPB rather than to determine the dielectric properties of these ceramics near the MPB in detail.

EXPERIMENTAL PROCEDURES

The polycrystalline samples with a general compositional formula:

$Pb_{1-z}La_z[Zr_xTi_y(Mo_{1/3},In_{2/3})_{1-(x+y)}]_{1-z/4}O_3$ with $z = 0.05$, $(x + y) = 0.95$ and $0.46 \leq x \leq 0.55$ were being prepared by a conventional dry ceramic method to form the solid solution of a composition that follows: $Pb_{0.95}La_{0.05}[Zr_xTi_{(0.95-x)}(Mo_{1/3},In_{2/3})_{0.05}]_{0.9875}O_3$. The reagent grade oxide of PbO , ZrO_2 , TiO_2 , La_2O_3 , MoO_3 and In_2O_3 were used as starting materials in a stoichiometric ratio. The powders were, first, ball-milled for twelve hours; and, then, calcined at $800^\circ C$ for two hours at the following heating and cooling rates: $2^\circ C/min$. After calcination, the mixture was, first, ball-milled for twenty- four hours; and then, dried and granulated with PVA as a binder. After drying, the powders were pressed into discs of a diameter of thirteen millimeters and of a thickness of about one millimeter. The compacted discs were being sintered at a temperature ranging from $1000^\circ C - 1180^\circ C$ for two hours in air. To prevent PbO volatilization from the pellets, a PbO atmosphere was controlled with a bed of $PbZrO_3$ powder placed in the vicinity of the pellets.

The X-ray diffraction (XRD, BRUCKER-AXS type D8 ADVANCE) was used to determine the crystalline phases present in the powder. The compositions of PZT phases were identified by the analysis of the peaks [(002)T, (200)R, (200)T] in the 2θ range $43^\circ - 47^\circ$. The tetragonal (T), rhombohedral (R) and tetragonal-rhombohedral phases were characterized and their lattice parameters were calculated. In order to ensure an accurate determination of the lattice parameters, the X-ray peaks were recorded gradually with 0.03° steps. Densities of sintered pieces were calculated from the sample dimensions and weights.

The dielectric response was measured at the frequency of 1kHz by using an automatic LCR meter at a temperature ranging from a room temperature to $400^\circ C$. The relationship between electrical properties and microstructures is reported and discussed.

RESULTS AND DISCUSSION

Phase structure

Sintered powders were examined by X-ray diffractometry to ensure phase purity, and to identify the crystal structure. The phases of the samples were detected using XRD (at room temperature) for several compositions given in Table 1. It can be seen that all the samples show pure perovskite structure, suggesting that La, Mo and In diffuse into the PZT lattice to form a solid solution. Fig.1 shows the XRD patterns (at room temperature) of the sintered PLZT-PMI samples with increasing Zr/Ti ratios. It is observed that a pure

perovskite phase is obtained. The tetragonal, rhombohedral and tetragonal–rhombohedral phases are identified by an analysis of the peaks [002(tetragonal), 200 (tetragonal), 200 (rhombohedral)] in the 2θ range of 43–47° correlated with JCPDS file number 33-0784 (T) and JCPDS file number 73-2022 (R). The splitting of the (002) and (200) peaks indicates that they are the ferroelectric tetragonal phase (FT), while the single (200) peaks consistent with the ferroelectric rhombohedral phase (FR). A transition from the tetragonal to the rhombohedral phase is observed as Zr/Ti ratio increases. Previously, a similar behavior was also observed with increasing Zr content in modified PZT based ceramics.

Table 1: Series of compositions and crystal structure

Sample	Crystal structure			
	1000°C	1100°C	1150°C	1180°C
Pb _{0.95} La _{0.05} [Zr _{0.46} Ti _{0.49} (Mo _{1/3} In _{2/3}) _{0.05}] _{0.9875} O ₃	T	T	-	-
Pb _{0.95} La _{0.05} [Zr _{0.47} Ti _{0.48} (Mo _{1/3} In _{2/3}) _{0.05}] _{0.9875} O ₃	T+R	T	T	-
Pb _{0.95} La _{0.05} [Zr _{0.49} Ti _{0.46} (Mo _{1/3} In _{2/3}) _{0.05}] _{0.9875} O ₃	T+R	T+R	T	T
Pb _{0.95} La _{0.05} [Zr _{0.50} Ti _{0.45} (Mo _{1/3} In _{2/3}) _{0.05}] _{0.9875} O ₃	T+R	T+R	T+R	T+R
Pb _{0.95} La _{0.05} [Zr _{0.51} Ti _{0.44} (Mo _{1/3} In _{2/3}) _{0.05}] _{0.9875} O ₃	T+R	T+R	T+R	T+R
Pb _{0.95} La _{0.05} [Zr _{0.52} Ti _{0.43} (Mo _{1/3} In _{2/3}) _{0.05}] _{0.9875} O ₃	T+R	T+R	R	R
Pb _{0.95} La _{0.05} [Zr _{0.54} Ti _{0.41} (Mo _{1/3} In _{2/3}) _{0.05}] _{0.9875} O ₃	T+R	T+R	R	-
Pb _{0.95} La _{0.05} [Zr _{0.55} Ti _{0.40} (Mo _{1/3} In _{2/3}) _{0.05}] _{0.9875} O ₃	R	R	-	-

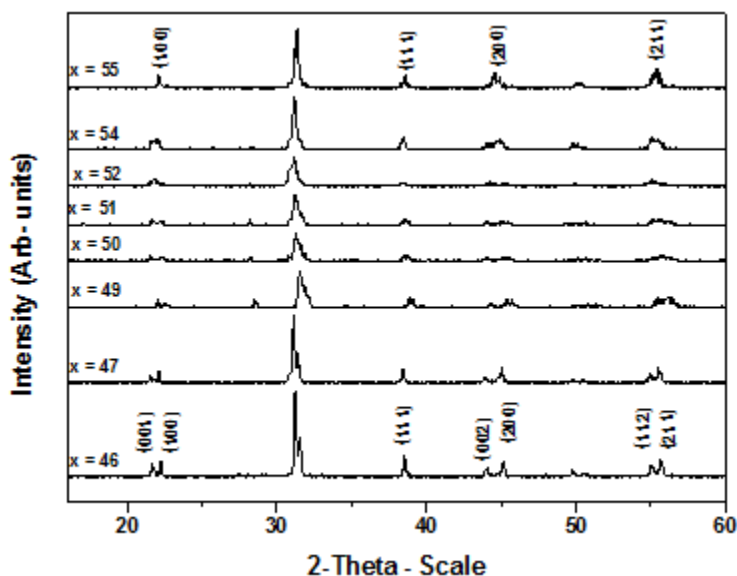


Figure 1: XRD patterns of Pb_{0.95}La_{0.05}[Zr_xTi_(0.95-x)(Mo_{1/3}In_{2/3})_{0.05}]_{0.9875}O₃ system sintered at 1180°C for 2 h, with 0.46 ≤ x ≤ 0.55

The multiple peak separation method was used to estimate the relative fraction of coexisting phases by which the relative phase fraction M_R and M_T were then calculated using the following Equations (1) and (2) [8]:

$$M_R = \frac{I_{R(200)}}{I_{R(200)} + I_{T(002)} + I_{T(200)}} \quad (1)$$

$$M_T = \frac{I_{T(002)} + I_{T(200)}}{I_{R(200)} + I_{T(002)} + I_{T(200)}} \quad (2)$$

Where $I_{R(200)}$ is the integral intensity of the (200) reflection of the rhombohedral phase and $I_{T(200)}$ and $I_{T(002)}$ are the integral intensities of the (200) and (002) reflections of the tetragonal phase, respectively. A

transition from tetragonal to rhombohedral phase is observed as Zr/Ti ratio increases. With increasing Zr/Ti ratio, tetragonal relative fraction decreases and rhombohedral relative fraction increases.

Analysis of the relative phase fractions in the PLZT-PMI ceramics indicates that the tetragonal and rhombohedral phases coexist in the composition range of $0.49 < x < 0.52$ as shown in Fig. 2. The co-existence of tetragonal and rhombohedral phases has, therefore, to be attributed to the first order nature of the MPB, this is marked contrast to the proposition of Kakegawa and al. [9,10] that the coexistence is invariably due to compositional fluctuations.

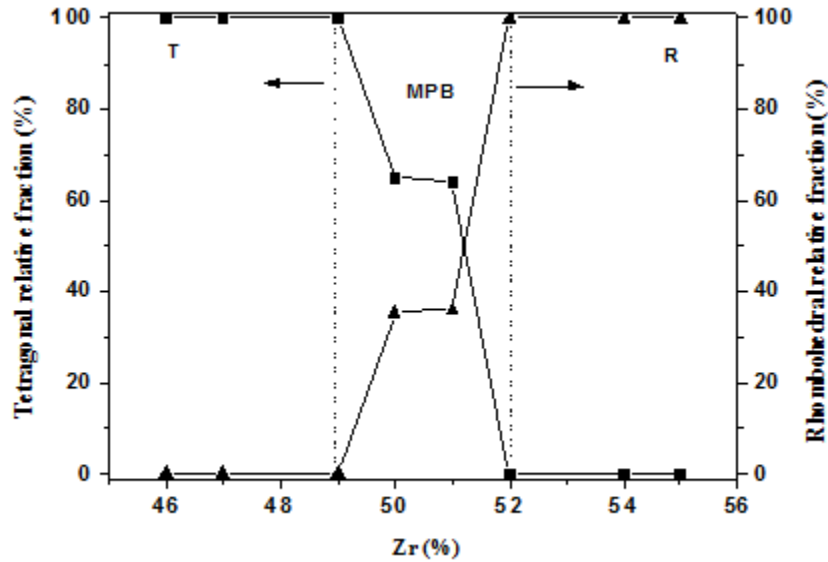


Figure 2: Variation of the relative content of the tetragonal and rhombohedral phases with different Zr% in the $Pb_{0.95}La_{0.05}[Zr_xTi_{(0.95-x)}(Mo_{1/3}In_{2/3})_{0.05}]_{0.9875}O_3$ (for a sintering temperature about 1180°C).

Fig. 3. shows the dependences of the measured density of the PLZT-PMI ceramics as a function of sintering temperature. The measured densities of the PLZT-PMI samples increase significantly with increasing sintering temperature achieving a maximum value at 1150°C and then decrease. From this figure, it was concluded that optimal sintering temperature for all samples was 1150 °C. The optimum sintering temperature depends on several factors such as the addition of impurities, the rate of heating, time of thermal treatment and protecting atmosphere.

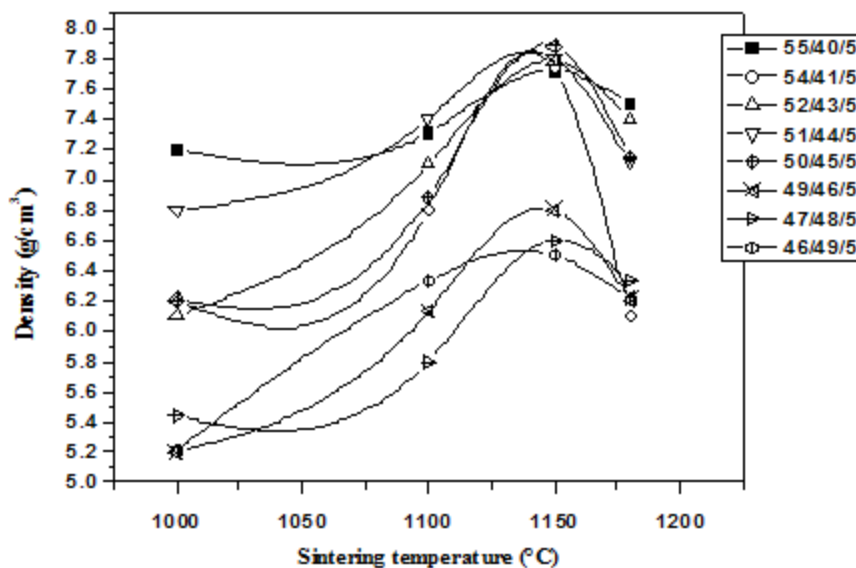


Figure 3: Density of PLZT-PMI ceramics with different Zr/Ti ratios as a function of sintering temperature

Changes in the density of different samples of PLZT-PMI sintered at 1150°C depending on the rate of Zr is shown in Fig. 4. The shape of the curve shows that the density increases with the increase of Zr concentration until a maximum value of 7.88g/cm³ (98.50% of theoretical density) at Zr = 50% (sample No. 4) and then it decreases.

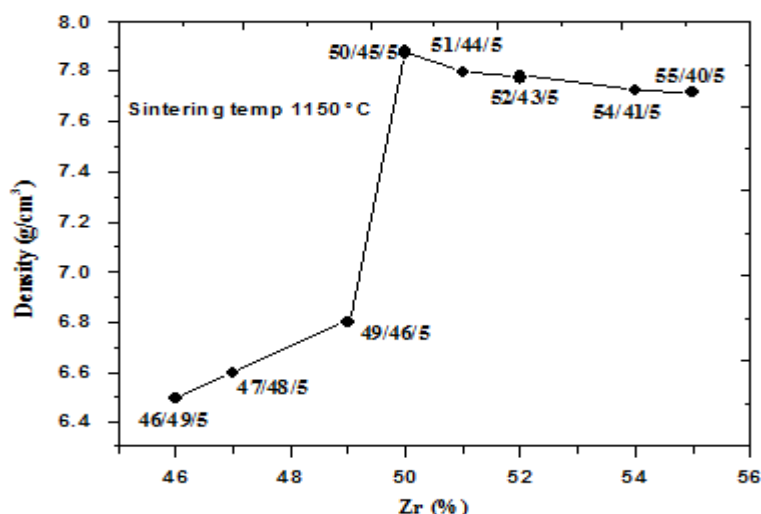


Figure 4: Density of PLZT-PMI ceramics sintered at 1150°C according to the variation of Zr %

Table 2 shows the lattice parameter values of a and c axes for each PLZT–PMI composition calculated from the XRD patterns. It can be seen that the lattice structure changes from the tetragonal to the rhombohedral phase as the ratio of Zr to Ti increases. The variation of these parameters is related to the distortion of the tetragonal structure defined by the c_T/a_T ratio (Tab. 2), which decreases with increasing Zr content, also confirming the occurrence of phase transition from tetragonal to rhombohedral symmetry. The rhombohedral lattice parameter a_R appears to oscillate between 4.0700 and 4.0820 Å. The influence of the Zr/Ti ratio on the lattice structure can be explained by the difference between the ionic rays of Zr and Ti (0.72 and 0.605 Å, respectively) [11].

Table 2: Comparison of crystal system (CS) and lattice parameters of PLZT-PMI ceramics sintered at 1180°C.

Zr/Ti ratio	CS	Lattice parameters (Å)			c/a
		$a_T = b_T$	c_T	a_R	
46/49	T	4.0375	4.1300	-	1.0229
47/48	T	4.0525	4.1325	-	1.0197
49/46	T	4.0625	4.1312	-	1.0169
50/45	T + R	4.0470	4.1100	4.0700	1.0155
51/44	T + R	4.0500	4.1080	4.0650	1.0143
52/43	R	-	-	4.0710	-
54/41	R	-	-	4.0750	-
55/40	R	-	-	4.0820	-

Dielectric properties

The temperature dependence of the dielectric constant for $Pb_{0.95}La_{0.05}[Zr_xTi_{(0.95-x)}(Mo_{1/3}In_{2/3})_{0.05}]_{0.9875}O_3$ ternary ceramics at 1 KHz (sintered at 1150°C) is shown in Fig. 5. It is observed in all the compositions as the temperature increase due to interfacial polarization becoming more dominant compared to the dipolar polarization [12]. After a certain temperature reached, the dielectric constant decreases due to the phase transition from ferroelectric to paraelectric. The transition temperature is called Curie temperature (T_c) which was obtained from $|d\epsilon_r/dT|$ versus temperature plot and those values are given in Table 3. We have observed that, the T_c decreases with the Zr concentration up to $x = 0.52$. Although we have observed increase of T_c for $y = 0.54$ and $x = 0.55$. It is due to the variation of the lattice parameters, and bond lengths.

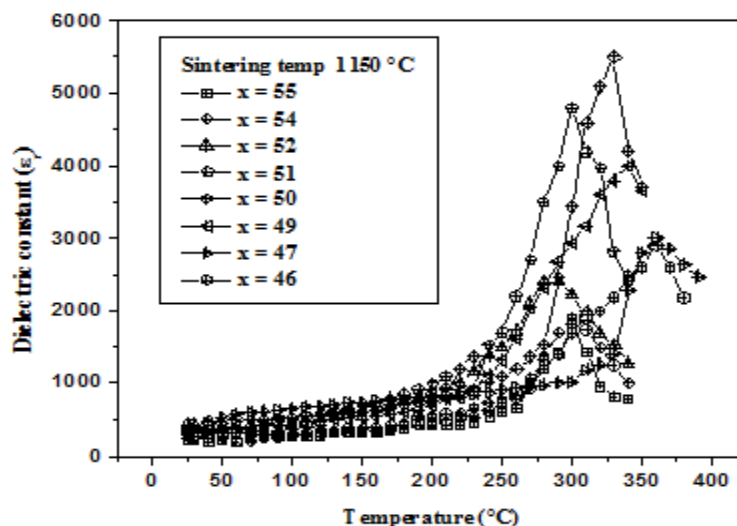


Figure 5: Temperature dependence of the dielectric constant for $\text{Pb}_{0.95}\text{La}_{0.05}[\text{Zr}_x\text{Ti}_{(0.95-x)}(\text{Mo}_{1/3}\text{In}_{2/3})_{0.05}]_{0.9875}\text{O}_3$ ternary ceramics sintered at 1150°C (1kHz)

Table 3: Dielectric data of the sample $\text{Pb}_{0.95}\text{La}_{0.05}[\text{Zr}_x\text{Ti}_{(0.95-x)}(\text{Mo}_{1/3}\text{In}_{2/3})_{0.05}]_{0.9875}\text{O}_3$ ternary ceramics sintered at 1150°C for $x = 0.46 - 0.55$ (1kHz)

Zr content (mol %)	T_C ($^\circ\text{C}$)	Dielectric constant ϵ_r (at T_C)
46	360	2900.848
47	354	3062.299
49	342	3987.131
50	335	5413.583
51	305	4797.671
52	285	2518.280
54	292	1902.310
55	300	1798.772

The variation of dielectric constant with frequency for $\text{Pb}_{0.95}\text{La}_{0.05}[\text{Zr}_x\text{Ti}_{(0.95-x)}(\text{Mo}_{1/3}\text{In}_{2/3})_{0.05}]_{0.9875}\text{O}_3$ ternary ceramics is shown in Fig.6. The plots show that the dielectric constant decreases with an increase in frequency, showing dispersion in lower frequency rang [13]. It attains a constant value and remains independent of frequency. Thereafter, all the samples reveal dispersion due to Maxwell-Wagner [14, 15] type interfacial polarization in agreement with Koop's phenomenological theory [16]. The high value of dielectric constant observed at lower frequencies can be explained on the basis of space charge polarization due to heterogeneous in structure like impurities, porosity and grain structure [17].

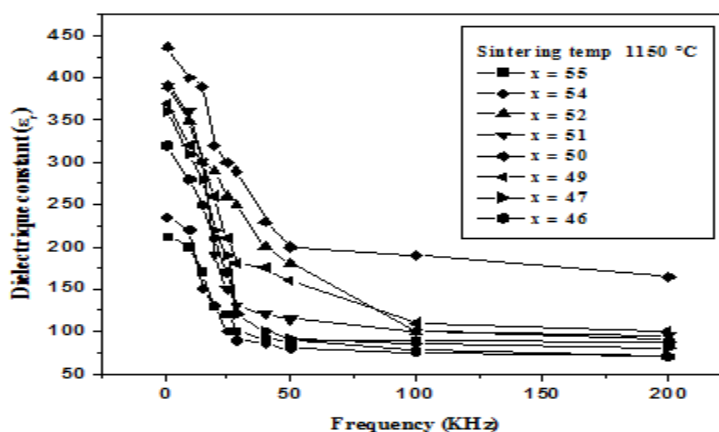


Figure 6: Variation of dielectric constant with frequency for $\text{Pb}_{0.95}\text{La}_{0.05}[\text{Zr}_x\text{Ti}_{(0.95-x)}(\text{Mo}_{1/3}\text{In}_{2/3})_{0.05}]_{0.9875}\text{O}_3$ ceramics sintered at 1150°C .

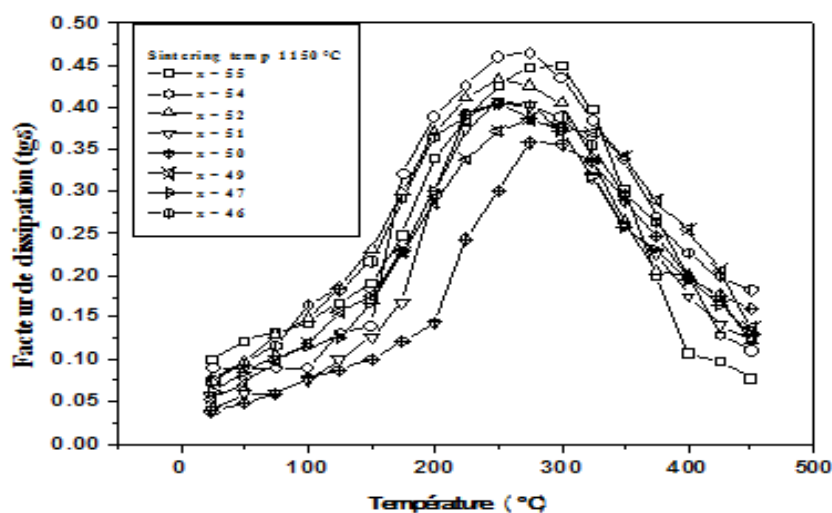


Figure 7: Dissipation factor according to the variation of composition and Temperature for $\text{Pb}_{0.95}\text{La}_{0.05}[\text{Zr}_x\text{Ti}_{(0.95-x)}(\text{Mo}_{1/3}\text{In}_{2/3})_{0.05}]_{0.9875}\text{O}_3$ ternary ceramics sintered at 1150°C (1kHz)

Fig.7 plots the temperature dependence of the dissipation factor behavior for the $\text{Pb}_{0.95}\text{La}_{0.05}[\text{Zr}_x\text{Ti}_{(0.95-x)}(\text{Mo}_{1/3}\text{In}_{2/3})_{0.05}]_{0.9875}\text{O}_3$ ternary ceramics sintered at 1150°C measured at 1kHz. All the samples within the investigated temperature range ($T^\circ\text{C} = 25- 450$) have dissipation factors $< 47\%$. At room temperature (25°C) the dissipation factor show the lower values of 3.92% for the composition with $x = 0.50$. This lower value is attributed to the high density and uniform microstructure.

CONCLUSION

In this study, ceramics in the $\text{Pb}_{0.95}\text{La}_{0.05}[\text{Zr}_x\text{Ti}_{(0.95-x)}(\text{Mo}_{1/3}\text{In}_{2/3})_{0.05}]_{0.9875}\text{O}_3$ ternary system (with $0.46 \leq x \leq 0.55$) were successfully prepared by a solid- state mixed-oxide technique. The phases of the sintered samples were examined by X-ray diffractometry. The XRD results reveal that an MPB with the co-existence of the rhombohedral and the tetragonal for the ceramics lies in the range of $x = 0.50 - 0.51$. The lattice parameters a_T and c_T of the tetragonal structure and a_R of the rhombohedral structure were found to change when composition is modified. The $\text{Pb}_{0.95}\text{La}_{0.05}[\text{Zr}_{0.50}\text{Ti}_{0.45}(\text{Mo}_{1/3}\text{In}_{2/3})_{0.05}]_{0.9875}\text{O}_3$ ceramics sintered at 1150°C exhibit good dielectric properties: $\epsilon_r = 5413.583$, $\tan\delta = 0.0392$ and $T_c = 335^\circ\text{C}$. This means that this system is a promising candidate for dielectric applications.

REFERENCES

- [1] Jaffe B, Cook WR and Jaffe H. Piezoelectric Ceramics, Academic Press, NewYork,1971;pp. 135-171.
- [2] Haertling GH. J Am Ceram Soc 1999; 82: 797-818.
- [3] Moulson AG and Herbert JM. Electroceramics, Second ed, John Wiley & Sons, Chichester, 2003.
- [4] Guiffard B, Boucher E, Lebrun L, Guyomar D. Mater Sci Eng 2007; B137: 272–277.
- [5] Wei Hng, Q. and Hoon, H. Chem And Phys 2002; 75: 151–156.
- [6] Qi Tan, Z Xu, Jie-Fanfg Li, and Dwight Viehland. J Appl Phys 1996;80: 5866-74.
- [7] Cross LE, Setter N, Colla EL. Ferroelectric Ceramics-Tutorial Review Theory, Processing and Applications, Birkhauser Verlag Basel 1993;1.
- [8] Haertling GH and Land CE. J American Ceram Soc 1971; 54:1-11.
- [9] Kakegawa K, Mohri J, Shrasaki X and Takahaashi K. J American Ceram Soc 1982; 65: 515-519.
- [10] Hammer W and Hoffmann MJ. J Electroceram 1998; 2: 75- 84.
- [11] Chih-Yen Chen, Yi Hu, Hur-Lon Lin, Wan-Yi Wei. Ceramics Int 2007; 33:263–268.
- [12] Kittel C, Wiley J, Inc S. Introduction to Solid State Physics, New York/Singapore 2006.
- [13] Shannigrahi SR, Tay FE H, Yao K, Choudhary RN P. J European Ceram Soc 2004;24:163-170.
- [14] Maxwell J.C. Electricity and Magnetism, Oxford University Press, London, 1973.
- [15] Wagner KW. Ann Physics 1993; 40:818.
- [16] Koops CG. Physical Rev 1951; 83: 121-124.
- [17] Upadhyay S and Omprakash D. Bull Mater Sci 1996; 19: 513-525.